

THIS DOCUMENT IS PART OF A NEW BOOK, IT IS BROUGHT TO YOU FREELY BY THE OPEN ACCESS JOURNAL MATERIALS AND DEVICES

Publication date: 2021, january 14th

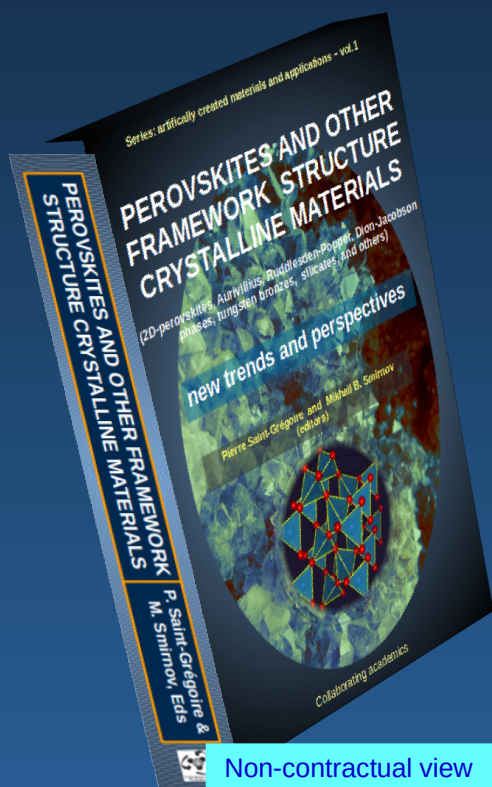
The book,
**“PEROVSKITES AND OTHER FRAMEWORK
STRUCTURE MATERIALS**

(2D-perovskites, Aurivillius, Ruddlesden-Popper, Dion-Jacobson phases, tungsten bronzes, clays, and others)

New trends and perspectives”

(editors P. Saint-Grégoire and M.B Smirnov)

Is a collective volume of 800 pages with **76 authors** and **26 chapters** on recent developments and hot subjects, divided into two parts:



A. Fundamental aspects and general properties

B. Elaborated materials and applied properties

Available in 3 formats:

- Ebook
- printed softcover, black & white
- printed hardcover, color.



Go to the Book(click)

Non-contractual view

Chap. 14 : The effect of an AC electric field on the dielectric properties of $\text{Pb}(\text{Mg}_{1/3}\text{Nb}_{2/3})\text{O}_3$ ceramic

E. C. Lima (1), J.D.S. Guerra (2), E.B. Araujo (3)

(1) Universidade Federal do Tocantins, Porto Nacional, Brazil

(2) Grupo de Ferroelétricos e Materiais Multifuncionais, Instituto de Física, Universidade Federal de Uberlândia, Brazil

(3) Departamento de Física e Química, Faculdade de Engenharia de Ilha Solteira, Universidade Estadual Paulista, Ilha Solteira, Brazil

Corresponding author: eltonlima@uft.edu.br

Abstract: The dynamic dielectric response of $\text{Pb}(\text{Mg}_{1/3}\text{Nb}_{2/3})\text{O}_3$ ceramic was experimentally studied as a function of the E_{AC} amplitude field. An increase in real dielectric permittivity was obtained by increasing the applied electrical field within the investigated temperature range for frequencies below 10 kHz. The temperature of maximum dielectric permittivity and freezing temperature decreased with an increase in E_{AC} . Nonlinear permittivity was studied and found to behave similarly to freezing temperature. A statistical model was used to fit the dielectric dispersion of real dielectric permittivity with temperature and frequency. The results are discussed in terms of different factors' contributions to dielectric permittivity under different E_{AC} field conditions.

Keywords: PMN, NONLINEAR DIELECTRIC PROPERTIES, AC ELECTRIC FIELD.

Cite this paper: E. C. Lima, J.D.S. Guerra, E.B. Araujo, OAJ Materials and Devices, vol 5(2) – chap No14 in “*Perovskites and other framework structure crystalline materials*”, p425 (Coll. Acad. 2021) – DOI:10.23647/ca.md20201706

I. Introduction

Relaxors are a unique class of materials in which dielectric permittivity depends on the frequency of the applied electric field [1, 2]. Smolenskii and Agranovskaya first discovered the relaxor behavior of $\text{Pb}(\text{Mg}_{1/3}\text{Nb}_{2/3})\text{O}_3$ (PMN) in the late 1950s [3]. Relaxors exhibit high dielectric constants, low hysteresis, and large electromechanical deformations, and they are an important part of technological materials that are commonly used to manufacture actuators, transducers, and sensors. Recently, scholars have focused on relaxors' electromechanical properties and debated the relationship between local structural heterogeneity and their extraordinary electromechanical properties [4].

Many review studies have pointed out the main differences between properties in normal ferroelectrics and relaxors [5, 6]. A high remaining polarization characteristic of a normal ferroelectric is a manifestation of a cooperative ferroelectric phenomenon. Differently, in relaxors materials, the behavior of hysteresis is characterized by the so-called slim loop, with low remaining polarization values and a narrow coercive field interval. Another important characteristic of ferroelectrics is to present a decrease in saturation or remaining polarization with increasing temperature and vanish at the Curie transition temperature. In contrast, relaxors persist in presenting polar regions well above the maximum permittivity temperature. As a result, the dependence of dielectric permittivity on temperature exhibits a large peak with maximum permittivity value at temperature T_m which is strongly dependent on the frequency of the probe field.

It is now commonly accepted that polar nanoregions (PNRs) are responsible for the extraordinary relaxor properties of relaxor ferroelectrics. Heterogeneity was believed to arise due to a positional disorder on the B-site cation in the ABO_3 perovskite-type ferroelectrics, as when cooled from the paraelectric phase, relaxor materials may have vacancies or imperfections that could be sources of random electric fields [7]. The quenching of field fluctuations upon cooling enabled the emergence of PNRs, as experimentally found with a deviation from the linear dependence of the refractive index by Burns et al. [8]. The temperature at which this occurs in PMN, 620 K, is called the Burns temperature. In fact, the dependence of the size of the PNRs on temperature has been studied in the PMN with diffuse scattering and it has been shown that these nanoregions increase during cooling below Burns' temperature [9]. Recently, studies based on dielectric, structural, lattice dynamical and piezoelectric measurements have demonstrated the weak and strong limits of the random electric field [10]. Various authors have suggested different explanations of relaxor behavior,

including the super-paraelectric model [1], dipolar glass model [11], random field model [12], breathing model [13], and spherical random-bond–random-field (SRBRF) model [14]. However, there are no conclusive explanations of the origin of PNRs. Thus, the purpose of this paper is to investigate the dielectric permittivity of PMN ceramics as a function of temperature and the E_{AC} electric field level based on the SRBRF model. A recently proposed approach based on a macroscopic and phenomenological statistical model was used to analyze diffuse phase transition behaviors in the investigated ceramic.

II. Experimental procedure

Dielectric measurements were performed on a PMN ceramic sample. PMN ceramic without secondary pyrochlore phase was obtained using the oxide precursor method, which produced a dense microstructure [15]. Dielectric permittivity was determined as a function of frequency and temperature, which ranged from 100 Hz to 1 MHz and 100–400 K, respectively. Field-dependent permittivity was measured using a weak probing AC electric field with a fixed amplitude. An E_{AC} field was supplied by an HP4284A LCR meter, which covered E_{AC} drive ranging from 0.004–0.4 kV/cm. Measurement was performed after discarding the remanence effects of the sample, taking into account the cooling cycle, and starting each run at 400 K.

III. Results and Discussion

Figure 1 shows the real (ϵ') and imaginary (ϵ'') dielectric permittivity of the PMN ceramic, which is measured at frequencies ranging from 1 kHz to 1 MHz and temperatures ranging from 100–400 K. Diffusive phase transition and frequency dispersion can be observed around the peaks of both the ϵ' and ϵ'' . The ϵ' gradually increases, and T_m increases with increasing probing frequency. As can be seen, dielectric dispersion is observed only around and below the temperature associated with the maximum dielectric permittivity ($T_m = 251$ K), which depends on the measurement frequency. As observed, the maximum real dielectric permittivity ($\epsilon'_m = 9029$ at 1 kHz) decreases with increasing frequency, while the maximum imaginary dielectric permittivity increases.

Figure 2 shows the dependence of the amplitude of the AC electric field on dielectric permittivity within the aforementioned temperature range at different measurement frequencies. The increase in dielectric permittivity measured around and below T_m is most pronounced at low frequencies. In addition, Figure 3(a) shows a decrease in T_m

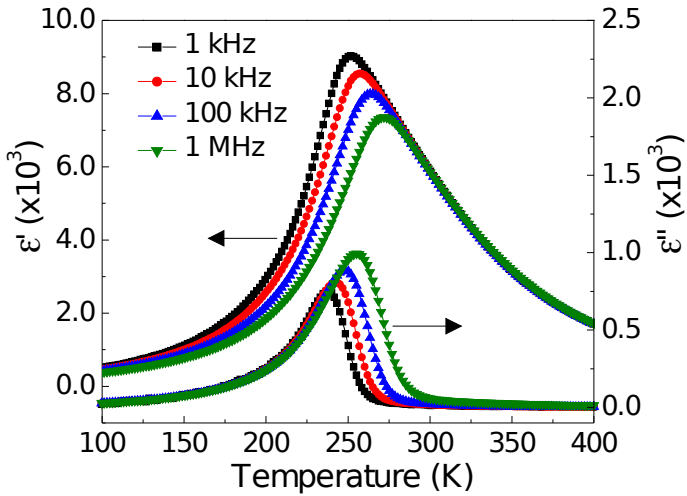


Figure 1: Temperature dependences of real and imaginary dielectric permittivity of PMN ceramic at various frequencies.

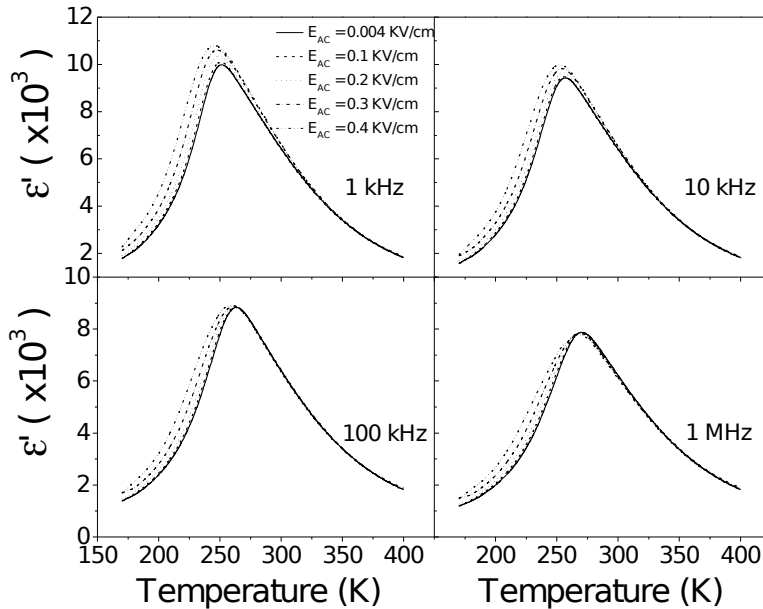


Figure 2: The temperature dependencies of the real parts of permittivity at different AC field levels and frequencies.

with increasing AC electric field amplitude. The increase in the magnitude of ϵ'_{max} is also greater at low frequencies. These results are consistent with some experimental observations for ceramics [16] and monocrystals [17, 18], and they agree with the results of Monte Carlo simulations for the relaxor materials [19].

The experiments showed a linear relationship between T_m and E_{AC} , but theoretically, a nonlinear relationship can be expected in a high-field regime. Interestingly, dielectric permittivity increases in small increments for the temperatures above T_m when measurements are made at a frequency of 1 KHz to 10 kHz. For frequencies greater than 100 kHz, the effect is less pronounced.

The relevance of the superparametric model to the experimental data indicates that interactions between polar clusters are crucial for explaining relaxor behavior. Viehland et al. [20] proposed a dipolar glass model in which cluster interactions are analogous to magnetic spin glasses and related dipolar glasses. In this model, individual clusters interact with each other through dipolar interactions. In the case of relaxors, such as PMN, the dispersion temperature of maximum permittivity was modeled according to the Vogel-Fulcher law given in Eq. (1), considering the relaxation in spin glasses [11]. More recently, super-Arrhenius behavior in glassy systems has been validated for relaxors, leading to a better understanding of the freezing temperature T_f of these materials [21].

$$\tau = \tau_0 \exp \left[\frac{E_a}{K_B (T_m - T_f)} \right] \quad (1)$$

Where τ_0 , E_a , and T_f are the fitting parameters. The Vogel-Fulcher relationship was validated for different AC electric field amplitudes. The fitting of this relationship with $E_{\text{AC}} = 0.4$ kV/cm can be seen in Figure 3(b). Figure 3(c) shows the electric field dependences for T_f and E_a . The freezing temperature undergoes a monotonic decrease with increasing E_{AC} , while the activation energy increases within the studied field range. Similar to T_m , T_f shows a slight change at lower AC field amplitudes and starts to decrease with E_{AC} over a certain threshold. As previously reported, T_f drops rapidly to 0 K when the AC field amplitude increases past the threshold value, resulting in destruction of the frozen state, in a PMN single crystal, the threshold field was around $0.15 \text{ kV}\cdot\text{cm}^{-1}$ [22]. In the present work, however, T_f drops to 18 K within the investigated AC field range. Previously, it was believed that changes in E_a and τ_0 with E_{AC} can indicate a fundamental change in relaxation as the relaxors are responding to the applied field (with phonon-based dynamics in a low field and domain-wall-like

dynamics in a high field) [23]. However, in this work, the value of T_r did not change significantly. Unlike the results Tyunina et al. [24] obtained for thin PMN films, which could be studied in a high-field regime, in this study the characteristic time (τ_0) was found to undergo major changes with an increase in the E_{AC} field.

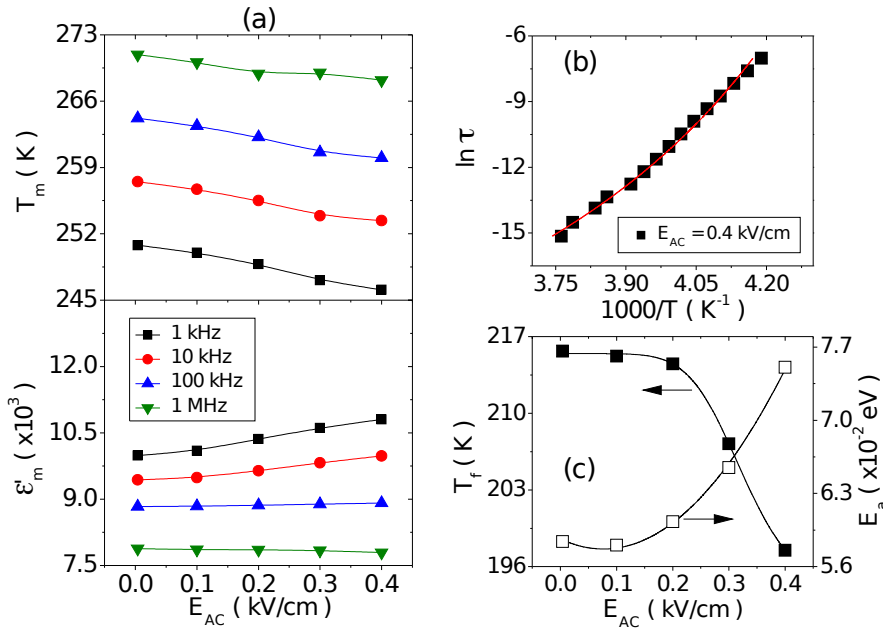


Figure 3: (a) Temperature of the real permittivity maximum (T_m), which corresponds to the position of the maximum $\epsilon'(T)$ of PMN ceramic as a function of the amplitude of the AC electric field at different frequencies. (b) Logarithm of relaxation time as a function of temperature corresponding to the maximum value of real permittivity. The line represents the best fit with Eq. (1). (c) Freezing temperature and activation energy as a function of the AC electric field amplitude. The lines help readers observe the results.

To understand the increase in dielectric permittivity with the increase of AC drive conditions, nonlinear permittivity was studied within the aforementioned temperature range at different frequencies. The nonlinear permittivity measured in the AC field is denoted as $\Delta \epsilon' = \epsilon'(E_{AC}) - \epsilon'(0)$, where $\epsilon'(E_{AC})$ and $\epsilon'(0)$ are the permittivity measured in an AC electric field and at the smallest possible amplitude, respectively.

In Figure 4, the nonlinear dielectric components are plotted as a function of

temperature at several AC field amplitudes and frequencies. At lower temperatures, the nonlinearity becomes positive at all field levels and frequencies, and the temperature that corresponds to the peak of the curve occurs below T_m and decreases with increasing AC electric field amplitude (see Figure 4[a]). The same behavior was observed for freezing temperature (see Figure 3[c]). These observations are consistent with the SRBRF model [14] and agree with previously performed computer simulations [19]. In the region above T_m , the nonlinear coefficient practically drops to zero for frequencies above 100 kHz and traverses a negative minimum around 280 K with a field of $E_{AC} = 0.4$ kV/cm. The increase in nonlinear permittivity with the amplitude of the electric field at a frequency of 1 kHz reflects the increase in real permittivity. Previous studies performed with PMN ceramic showed that the dielectric permittivity measured at 1 kHz reaches a maximum between 3 and 5 kV/cm at a temperature range of 209–253 K, and at a high temperature (293 K), large variation was not observed [25]. Other studies with PMN thin films found similar results [24].

To better understand the polarization mechanisms of the relaxors, we used a statistical model to fit the dielectric dependence to the temperature and amplitude of the electric field probe below and above T_m . Liu et al. [26] recently proposed a statistical model based on the assumption that a potential well of average depth (E_b), which relates to the size of PNRs, exists in relaxor materials. According to the model, the temperature dependence of dielectric susceptibility is proposed to be as follows:

$$\chi = \frac{\chi_1}{1 + \left| \frac{T - T_0}{\theta} \right|^\gamma} \cdot P_1(E_b, T) + \chi_2 \cdot [P_2(E_b, T)] \quad (2)$$

where γ is a critical exponent, T_0 is associated with the peak position of a moderate phase transition, θ is a parameter describing the width of the peak, χ_1 represents the group of dipoles subjected to thermal excitation, and χ_2 represents dipoles inside the potential well that contribute to constant susceptibility. To normalize the dipoles to unit volume, it is assumed that $P_1(E_b, T) = N_1(E_b, T)/N$ and $P_2(E_b, T) = [N - N_1(E_b, T)]/N$, with N representing the total number of dipoles.

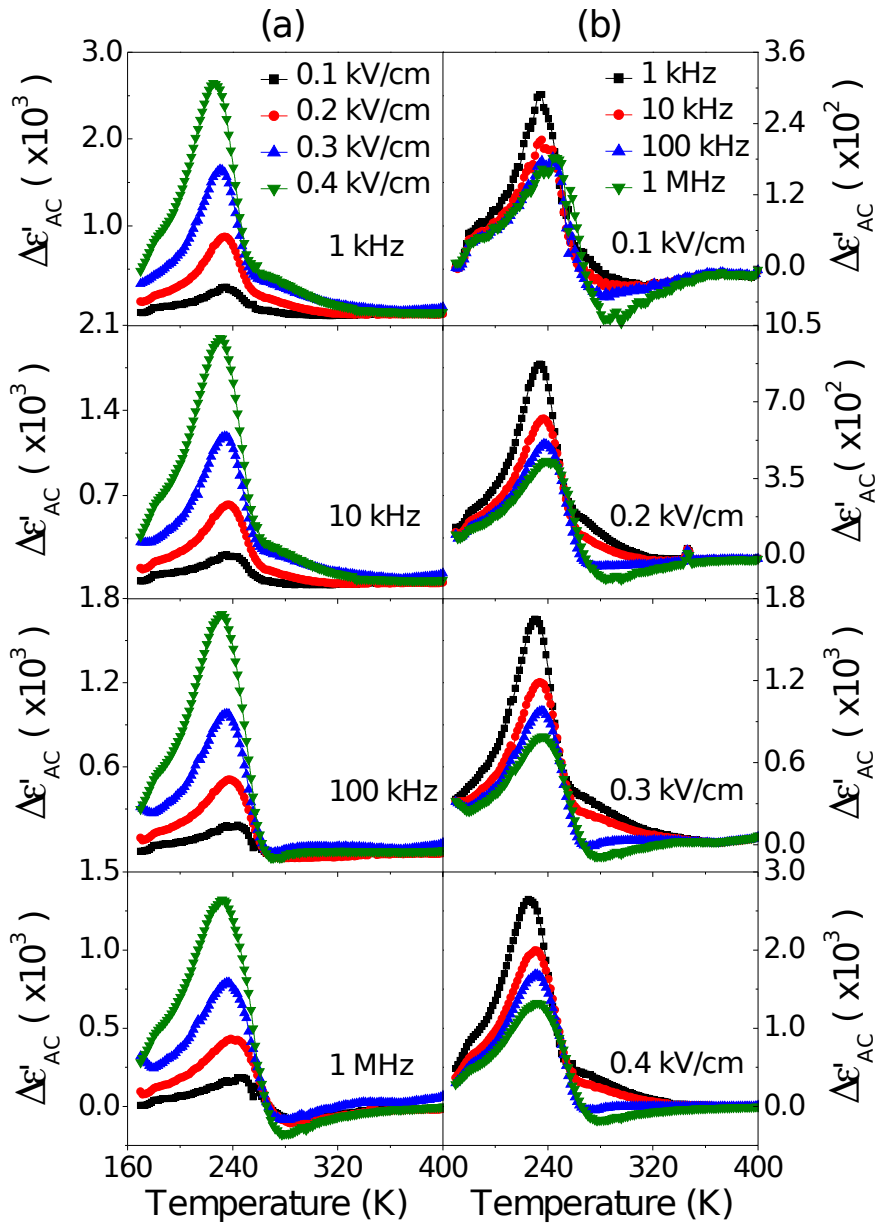


Figure 4: Temperature dependence of nonlinear dielectric permittivity for PMN ceramic (a) in different AC electric fields at selected frequencies and (b) at different frequencies in selected AC electric fields.

The kinetic energy of individual dipoles obeys the Maxwell-Boltzmann distribution, and the number of dipoles (N_1) with kinetic energy that exceeds E_b is given by the following equation:

$$N_1(E_b, T) = N \sqrt{\frac{4}{\pi}} \sqrt{\frac{E_b}{k_B T}} \exp\left(\frac{-E_b}{k_B T}\right) + N \operatorname{erfc}\left(\sqrt{\frac{E_b}{k_B T}}\right) \quad (3)$$

where k_B is the Boltzmann constant and erfc is the complementary error function. We used Eq. (2) to fit the $\epsilon'(T)$ of PMN ceramic with different AC electric fields and frequencies, and the results are shown in Fig. 5.

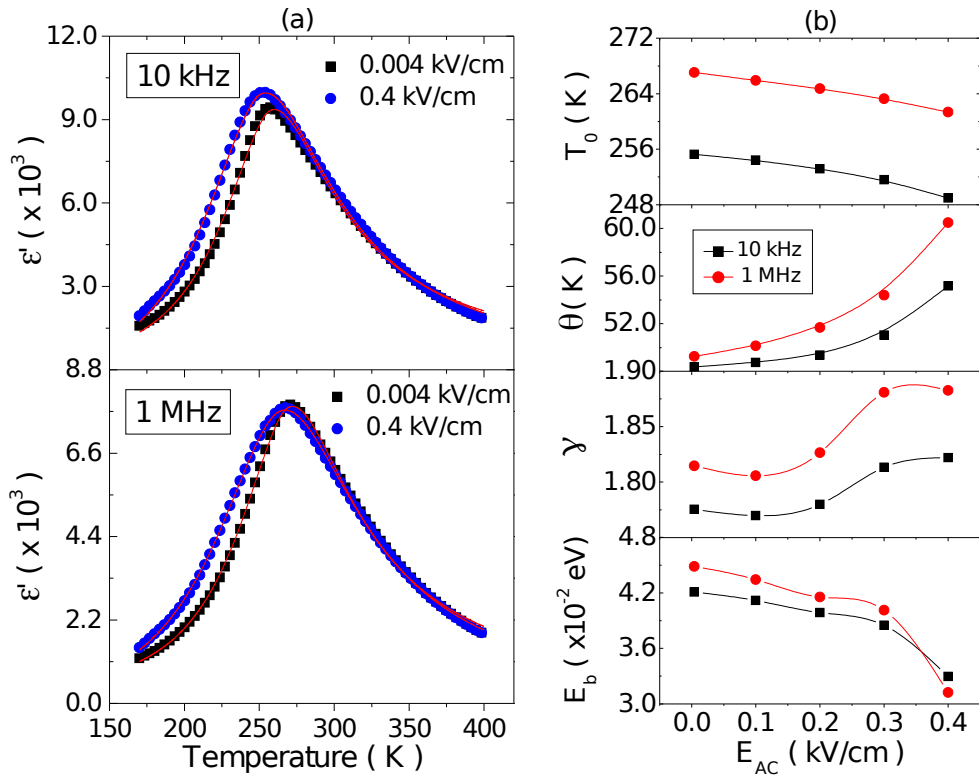


Figure 5: (a) Dielectric permittivity as a function of temperature at different AC field levels and frequencies. The lines represent the best fit with Eq. (2). (b) Fitting parameters of PMN ceramic permittivity obtained at different AC field levels at selected frequencies.

According to the best fittings with the statistical approach, the trends of change in parameters with respect to AC electric fields can be summarized as follows. First, χ_1 (27,000) was found to be higher than χ_2 (516) at $E_{AC} = 0.004$ kV/cm measured at 1 MHz. The same behavior was observed for the other fittings. As suggested by the model, $\chi_1 \gg \chi_2$ for Pb-based relaxors, indicating that dipoles outside the average potential well have a dominant effect on the dielectric response of Pb-based relaxors. Second, T_0 decreases when the electric field increases. Despite the distinction we made between the parameters T_m and T_0 , according to our fitting, the behavior of these parameters—as described in Figures 3(a) and 5(b)—are quite similar, with differences of 1–2%. Third, θ and γ increase when the electric field increases. A value of $\gamma=1$ indicates a “normal” ferroelectric phase transition, which is described by the Landau–Devonshire theory for ferroelectric phase transitions (first- or second-order phase transitions). A value of $\gamma=2$ represents a so-called diffuse phase transition [27]. Fourth, E_b decreases with increases in the AC drive electric field. It has been suggested that a decrease in E_b is responsible for the increase in dielectric dispersion of $Ba(Ti_{1-x}Zr_x)O_3$ ceramics in solid solutions when the system undergoes a continuous change from normal ferroelectrics to relaxors and the composition (x) increases from 0.1 to 0.4 [28]. Similarly, an increase in the electric field also led to an increase of the parameter θ . Computer simulations have shown that the size of PNRs in PMN increases during cooling below the Burns temperature [29], and experimental studies have shown the influence of temperature on the formation of PNRs [30]. Experimental studies by diffuse scattering in PMN revealed an increase in size of the PNRs during cooling below the Burns temperature [9]. However, experimental studies have not investigated the size behavior of PNRs with increasing AC drive. The bias field has drawn more attention from the scientific community, as a study based on combined experimental observations and phase-field simulations quantified the contributions of PNRs to the dielectric and piezoelectric properties of relaxor PMN–PT crystals [31].

IV. Conclusion

Dielectric measurements have been performed on PMN ceramic using various AC drive amplitudes and frequencies. Significant changes in the dielectric permittivity curves were observed with increasing drive. The freezing temperature behavior as AC drive increased agreed with the predictions of the SRBRF model. The peak temperature dependence of nonlinear permittivity was shown to exhibit similar behavior to the freezing

temperature based on the Vogel-Fulcher relationship. The freezing temperature undergoes a monotonic decrease with increasing E_{AC} , while the activation energy increases within the studied field range. A statistical model was used to understand and fit the dependence of dielectric permittivity with temperature below and above the maximum permittivity temperature. The obtained parameters were discussed in terms of the influence of increased AC electric field amplitude.

Acknowledgements:

We would like to express our gratitude to the CNPq, FAPEMIG, and FAPESP Brazilian agencies for financial support.

Complementary informations on authors:

e-mail: eltonlima@uft.edu.br, ORCID: 0000-0002-8534-3621.

Cite this paper: E. C. Lima, J.D.S. Guerra, E.B. Araujo, OAJ Materials and Devices, vol 5(2) – chap No14 in “*Perovskites and other framework structure crystalline materials*”, p425 (Coll. Acad. 2021) – DOI:10.23647/ca.md20201706

REFERENCES

1. L.E.Cross, *Ferroelectrics*, **vol.76**, p 241 (1987)
2. A.A.Bokov, Z.-G.Ye, *J. Mater. Sci.*, **vol.41**, p 31 (2006)
3. G.A.Smolenskii, A.I.Agranovskaya, *Sov. Phys.-Tech. Phys.*, **vol.3**, p 1380 (1958)
4. F.Li, S.J.Zhang, D.Damjanovic, L.Q.Chen, T.R.Shroud, *Adv. Funct. Mater.* **vol.28**, 1801504 (2018)
5. G.A.Samara, *J. Phys.: Condens. Matter*, **vol.15**, p R367–R411 (2003)
6. R.A.Cowley, S.N.Gvasaliya, S.G.Lushnikov, B.Roessli, G.M.Rotaru, *Advances in Physics*, **vol.60**, p 229 (2011)
7. W.Kleemann, *J. Mater. Sci.*, **vol.41**, p 129 (2006)
8. G.Burns, F.H.Dacol, *Solid State Commun.*, **vol.48**, p 853 (1983)

9. G.Xu, G.Shirane, J.R.D.Copley, P.M.Gehring, *Phys. Rev. B*, **vol.69**, p 064112 (2004)
10. D.Phelana, C.Stocka, J.A.Rodriguez-Rivera, S.Chia, J.Leão, X.Long, Y.Xie, A.A. Bokov, Z-G.Ye, P.Ganesh, P.M.Gehring, *Proc. Natl. Acad. Sci. U.S.A.*, **vol.111**, p 1754 (2014)
11. D.Viehland, S.J.Jang, L.E.Cross, M.Wuttig, *J. Appl. Phys.*, **vol.68**, p 2916 (1990)
12. V.Westphal, W.Kleemann, M.D.Glinchuk, *Phys. Rev. Lett.*, **vol.68**, p 847 (1992)
13. A.E.Glazounov, A.K.Tagantsev, *Ferroelectrics*, **vol.221**, p 57 (1999)
14. R.Pirc, R.Blinc, *Phys. Rev. B*, **vol.60**, p 13470 (1999)
15. C.A.Guarany, R.N.Reis, E.B.Araújo, C.T.Menezes, A.G.Souza Filho, J.M.Sasaki, J.Mendes Filho, *Ferroelectrics*, **vol.334**, p 147 (2006)
16. A.E.Glazounov, A.K.Tagantsev, D.A.J.Bell, *Ferroelectrics*, **vol.184**, p 217 (1996)
17. A.K.Tagantsev, A.E.Glazounov, *Phys. Rev. B*, **vol.57**, p 18 (1998)
18. D.S.Fu, H.Taniguchi, M.Itoh, S.Koshihara, N.Yamamoto, S.Mori, *Phys. Rev. Lett.*, **vol.103**, 207601 (2009)
19. Z.R.Liu, B.L.Gu, X.W.Zhang, *Phys. Rev. B*, **vol.62**, p 1 (2000)
20. D.Viehland, S.J.Jang, L.E.Cross, *Phys. Rev. B*, **vol.46**, p 8003 (1992)
21. R.Levit, D.A.Ochoa, J.C.Martinez-Garcia, J.E.Garcia, *J. Phys. D: Appl. Phys.*, **vol.52**, 505301 (2019)
22. E.V.Colla, S.M.Gupta, D.Viehland, *J. Appl. Phys.*, **vol.85**, p.362 (1999)
23. E.V.Colla, E.L.Furman, S.M.Gupta, N.K.Yushin, D.Viehland, *J. Appl. Phys.*, **vol.85**, p 1693 (1999)
24. M.Tyunina, J.Levoska, *Phys. Rev. B*, **vol.72**, 104112 (2005)
25. T.Tsurumi, K.Soejima, T.Kamiya, M.Daimon, *Jpn. J. Appl. Phys.*, **vol.33**, p 1959 (1994)
26. J.Liu, F.Li, Y.Zeng, Z.Jiang, L.Liu, D.Wang, Z.-G.Ye, C.-L.Jia, *Phys. Rev. B*, **vol.96**, 054115 (2017)
27. K.Uchino, S.Nomura, *Ferroelectrics*, **vol.44**, p 55 (1982)
28. L.Liu, S.Ren, J.Zhang, B.Peng, L.Fang, D.Wang, *J. Am. Ceram. Soc.*, **vol.101**, p 2408 (2018)
29. A.Al-Barakaty, S.Prosandeev, D.Wang, B.Dkhil, L.Bellaiche, *Phys. Rev. B*, **vol.91**, 214117 (2015)
30. G.Xu, G.Shirane, J.R.D.Copley, P.M.Gehring, *Phys. Rev. B*, **vol.69**, 064112 (2004)
31. F.Li, S.J.Zhang, T.N.Yang, Z.Xu, N.Zhang, G.Liu, J.J.Wang, J.L.Wang, Z.X.Cheng, Z.-G.Ye, J.Luo, T.R.Shrouf, L.Q.Chen, *Nat Commun*, **vol.7** 13807 (2016)